

3D ARTICULATED HAND TRACKING BY NONPARAMETRIC BELIEF PROPAGATION ON FEASIBLE CONFIGURATION SPACE

Tangli Liu, Wei Liang and Yunde Jia

*School of Computer Science&Technology, Beijing Institute of Technology, 5 South Zhongguancun Street
Haidian District, Beijing 100081, P. R. China*

Keywords: Articulated hand tracking, graphical model, NBP.

Abstract: An efficient articulated hand tracking method underlying the 3D graphical model from monocular image sequences is proposed in this paper. Due to the inaccurate dependences among the components of human hand leading to distorted estimates in previous work, we design a pertinence graphical model combined with domain-specific heuristics among the components of human hand describing the hand's 3D structure, kinematics, and dynamics. The proposed model decomposes multivariate, joint distributions into a set of local interactions among small subsets. The modular structure provides an intuitive language for expressing domain-specific knowledge about the variable relationships, and facilitates tracking each hand component independently. And then, we provide a novel belief propagation algorithm to inference in hand graphical model. The algorithm can accommodate an extremely broad class of potential functions besides the potentials appropriate for our model. The experimental results show the robustness and efficiency of tracking each hand component.

1 INTRODUCTION

Tracking unrestricted 3D human hand movement has fundamental importance for human-computer interaction (HCI). Articulated human hand tracking is inherently a very difficult problem due to: 1) high degree of freedom (about 27 degrees) of the articulated hand movement (Wu et al., 2005); 2) occlusion among hand components; 3) the posterior distribution of hand configuration is multimodal and spiky and so forth.

The existing methods for tracking hand motion could be divided into two categories. One is the appearance-based approach that estimates articulated motion states directly from images by learning the mapping from an image feature space to the hand configuration space. The other is the model-based approach that estimates articulated motion states by projecting a 3D model on to the image space and then compares the projections with the observations (Stenger et al., 2001; Wu et al., 2001; Isard and Blake, 1998). One advantage of the former is that real time tracking can be processed. However, large and dense reference images should be collected in

advance to get an accurate estimation. Also, effective learning or retrieval in a large image set is very demanding. The latter approach can provide an accurate estimation when a 3D model is well initialized, while inevitably perform searching in a high dimensional space.

The performance of a model-based tracker depends on the type of the used model. The tracking results are more accurate if the model is more complex enough. However, there is a trade-off between accurate modelling and efficient observation (Lin et al., 2002).

Fortunately, the natural human motion is often highly constrained and the motions among various joints are closely correlated (Chao et al., 1989). Till now some simple and closed form constraints have been found in biomechanics and applied to hand motion analysis (Tony et al., 2006), further investigations on the representations and utilizations of complex motion constraints and the configuration space have not yet been conducted. With the rich restrictions of hand motion, the intrinsic and feasible hand motion seems to be constrained within a subset (or the feasible configuration space) of original high DOF (degree of freedom) space. Once the feasible

configuration space is characterized, it could dramatically reduce the search space in hand configuration space.

Graphical models provide a powerful framework for specifying precise, modular descriptions of computer vision tasks and developing corresponding learning and inference algorithms. Inference algorithms for visual scenes must then be tailored to the high-dimensional, continuous variables and complex distributions. The graphical model decomposes multivariate, joint distributions into a set of local interactions among small subsets. The modular structure provides an intuitive language for expressing domain-specific knowledge about the variable relationships, and facilitates tracking each hand component independently. Recently, graphical models are widely used in tracking articulated objects such as human hand and body (Isard, 2003; Sigal et al., 2004; Frey et al., 1998). Sudderth et al. apply a graphical model describing the 3D hand structure, kinematics, and dynamics (Sudderth et al., 2004). This graph encodes global hand pose via the 3D position and orientation of several rigid components, and thus exposes local structure in a high-dimensional articulated model. The tracking problem is formulated as one of inference in a graphical model and belief propagation (Frey et al., 1998) can be used to estimate the pose of the hand at each time-step.

In this paper, we extract the occlusion constraints from the image cues and syncretize these relationships with the traditional restrictions for articulated human hand tracking. In section 4, the experimental results demonstrate our model can deal with self occlusion while tracking hand. Then, we provide a novel belief propagation algorithm to inference over hand graphical model. The algorithm can accommodate an extremely broad class of potential functions besides the potentials appropriate for our model.

Our work has three main contributions: 1) We introduce occlusion constraints into the existing models to allow graphical model-based hand tracking method handle the self-occlusion instance. 2) Novel potential functions appropriate for the proposed hand model are incorporated in the tracking process, thus leading to a very efficient computation. 3) We design a more efficient belief propagation method by embedding Continuously Adaptive Mean Shift (CAMSHIFT) algorithm in sampling procedure of NBP to focus the samples on the more likely locations. Moreover we use sequential density mode propagation in the feasible

configuration space derived from the above procedure to accelerate the efficiency of NBP remarkably.

2 A SELF-ASSEMBLING HAND MODEL

Human hand is composed of sixteen approximately rigid components: three phalanges or links for each finger and thumb, as well as the palm (Wu and Huang, 2001). Following Stenger's work (Stenger et al., 2001), we model each rigid body by cylinders with fixed size, as illustrated in figure 1(b) and the real hand image is showed by figure 1(a). These geometric primitives are well matched to the true geometry of the hand, and in contrast to 2.5D "cardboard" models (Wu et al., 2001), allow tracking from arbitrary orientations.

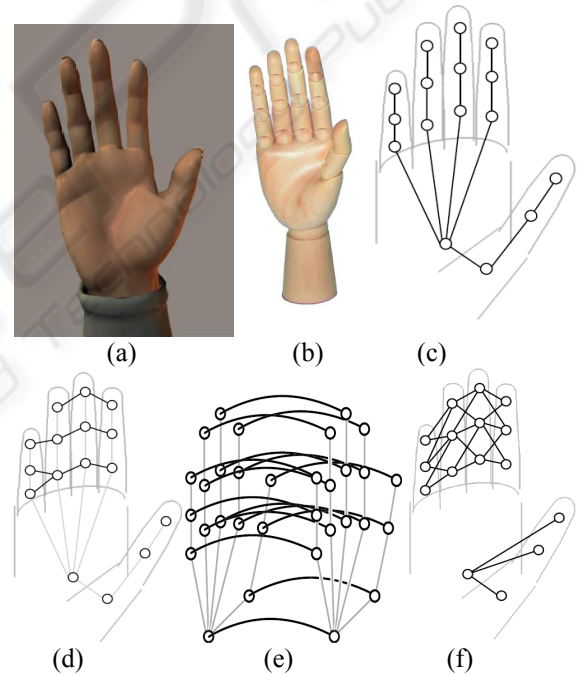


Figure 1: Self-assembling hand model: (a) human hand (b) cylinders with fixed size to represent each hand phalanx (c) kinematic constraints (d) structure constraints (e) temporal dynamics (f) occlusion relationships.

Each component has an associated configuration vector defining the component's position and orientation in 3D space. Placing each part in a global coordinate frame enables the part detectors to operate independently while the full hand is assembled by inference over the graphical model.

2.1 Kinematic Representation and Constraints

To determine the image evidence for a given hand configuration, the 3D position and orientation (or pose) of each hand component should be determined. As traditional graphical models, we assume the variables in a node are independent of those in non-neighbourhood. Each component/phalange is modelled by a cylinder having two fixed (person specific) and six estimated parameters. The fixed parameters $f_i = (L_i, W_i)$ correspond to the phalange's length, width respectively. The estimated parameters $e_i = (X_i, \theta_i)$ represent the configuration of the part i in a global coordinate frame where $X_i \in R^3$ and $\theta_i \in SO(3)$ are the 3D position of the proximal joint and the angular orientation of the part respectively. The rotations are represented by unit quaternions. The configuration of the whole hand is represented by $E = \{e_1, \dots, e_{16}\}$.

Let E_k be the set of all pairs of rigid bodies which are connected by joints, or equivalently the edges in the kinematic graph of figure 1(c). The kinematics constraints are written as

$$\psi_{i,j}^k(e_i, e_j) = \begin{cases} 1 & \text{if the } (e_i, e_j) \text{ is valid rigid body} \\ & \text{configuration associated with} \\ & \text{some setting of the angles of } (i, j) \\ 0 & \text{otherwise} \end{cases} \quad (1)$$

Viewing the component configurations as random variables, the following prior explicitly enforces all constraints implied by the original joint angle

$$p_K(x) \propto \prod_{(i,j) \in E_k} \psi_{i,j}^k(x_i, x_j) \quad (2)$$

It is noticeable that the position and orientation of each finger are determined by an independent set of joint angles. So, $\psi_{i,j}^k(\cdot)$ is statistically independent.

The kinematics constraints avoid irregular hand configuration.

2.2 Structural Constraints

Obviously, the hand's joint angles are coupled because different fingers can never occupy the same physical volume. As proposed by Sudderth et al. (Sudderth et al., 2004), the structure constraints $\psi_{i,j}^s(e_i, e_j)$ are written as

$$\psi_{i,j}^s(e_i, e_j) = \begin{cases} 1 & \|e_i(X) - e_j(X)\| > \delta_{i,j} \\ 0 & \text{otherwise} \end{cases} \quad (3)$$

where $\delta_{i,j}$ is a threshold determined by fixed parameters f_i and f_j . So the structural prior is

$$p_s(x) \propto \prod_{(i,j) \in E_s} \psi_{i,j}^s(x_i, x_j) \quad (4)$$

E_s describes those pairs of bodies which are likely to intersect (Figure 1(d)). This constraint prevents different fingers from tracking the same image data.

2.3 Temporal Dynamics

The hand configuration at time t is denoted by x_t , and its history is $X_t = \{x_1, \dots, x_t\}$. Similarly the set of image features at time t is z_t with history $Z_t = \{z_1, \dots, z_t\}$. All these methods estimate x_{t+1} at time $t+1$ through Bayesian formulation.

$$p(x_{t+1} | Z_{t+1}) \propto p(z_{t+1} | x_{t+1}) p(x_{t+1} | Z_t) \quad (5)$$

where $p(x_{t+1} | Z_t) = \int_{x_t} p(x_{t+1} | x_t) p(x_t | Z_t) dx_t$. A general assumption is made for the probabilistic framework that the object dynamics form a temporal Markov chain. So the new state is conditioned directly only on the immediately preceding state, independent of the earlier history. And we assume that for each component, $p(x_{t+1} | x_t)$ represents our dynamical model of hand motion which obeys the Gaussian distribution.

2.4 Occlusion Constraints

We employ edge (Figure 2) and color cues to construct the observation model. Edges and colors should be transformed into likelihood measurements consistently with the hand constraints described above. We utilize both color and edge cues by selecting the technique of histograms, therefore the resulting probability distribution forms through a Bayesian formulation are represented as $p_e(U | x)$ and $p_c(U | x)$ (x denotes 3D hand pose and U , the image). We let u represent the color and intensity of an individual pixel, and $U = \{u \in \eta\}$ the full image defined by some rectangular pixel lattice η .

In this paper, the cylinder model of each hand component with the hypothetical configuration is projected in the real image plan. A gradient based edge detection mask is used to detect edges of the real image. For the likelihood described by occlusion-sensitive color and edge cues, the occlusion masks k must be chosen consistently

with the 3D hand pose x . These consistency constraints can be expressed by the following potential function

$$O(x_j, k_{i(u)}, x_i) = \begin{cases} 0 & \text{if } x_j \text{ occludes } x_i, u \in \pi(x_j), \\ & \text{and } k_{i(u)} = 1 \\ 1 & \text{otherwise} \end{cases} \quad (6)$$

$$k_i = \{k_{i(u)} | u \in \eta\}, \quad k_{i(u)} = \begin{cases} 0 & \text{if pixel } u \text{ in the projection} \\ & \text{of } i \text{ is occluded by other part} \\ 1 & \text{otherwise} \end{cases} \quad (7)$$

$\pi(x)$ denotes the set of pixels in the projected silhouette of 3D hand pose x .

The following potential encodes all of the occlusion relationships between rigid bodies and

$$\psi_{i,j}^O(x_i, k_i, x_j, k_j) = \prod_{u \in E} O(x_j, k_{i(u)}, x_i) O(x_i, k_{j(u)}, x_j) \quad (8)$$

These occlusion constraints exist between all pairs of nodes. However, as with the structural prior, we enforce only those pairs (Figure 1(f)) most prone to occlusion

$$p_{O(x,z)} \propto \prod_{(i,j) \in E_O} \psi_{i,j}^O(x_i, k_i, x_j, k_j) \quad (9)$$



Figure 2: Feature extraction. A real image is on the left, the resulting edge is on the right.

3 EFFICIENT BELIEF PROPAGATION ON FEASIBLE CONFIGURATION SPACE

3.1 Potential Functions

We have shown that a local representation of the geometric hand model's configuration x^t allows $p(x^t | Z^t)$, the posterior distribution of the hand model at time t given observed image z^t , to be expressed as

$$\begin{aligned} p(x^t | Z^t) &\propto p_K(x^t) p_S(x^t) p_e(Z^t | x^t, k^t) p_e(Z^t | x^t, k^t) \\ &= p_K(x^t) p_S(x^t) \prod_{i=1}^{16} p_c(Z^t | x_i^t, k_i^t) p_e(Z^t | x_i^t, k_i^t) \end{aligned} \quad (10)$$

When τ video frames are observed, the overall posterior distribution then equals

$$p(x | Z) \propto \prod_{t=1}^{\tau} p(x^t | Z^t) p_T(x^t | x^{t-1}) \quad (11)$$

Equation (11) is an example of a pairwise Markov random field, which takes the following general form

$$p(x | Z) \propto \prod_{(i,j) \in E} \psi_{i,j}(x_i, x_j) \prod_{i \in \Theta} \psi_i(x_i, Z) \quad (12)$$

Here, the nodes Θ correspond to the sixteen components of the hand model at each time point, and the edges E arise from the union of the graphs encoding kinematic, structural, and temporal constraints. Visual hand tracking can thus be posed as inference in graphical model. Thus, the resulting distribution probability are factored into two potential types: one can be considered as the relationships between two neighbouring nodes in the hyper graph which encodes kinematic, structural, and temporal constraints, another can be viewed as the node's local information at each point at time including image cues and occlusion instances. This framework is general for tracking articulated objects besides human hand by varying the potential functions.

3.2 NBP Embedded With CAMSHIFT

Inferring the hand pose in our framework is defined as estimating belief in the graphical model. To cope with the continuous 6D parameter space of each hand component, the non-Gaussian conditionals between nodes, and the non-Gaussian likelihood, we develop an efficient nonparametric belief propagation algorithm underlying the work in (Sudderth et al, 2004).

Each NBP message update involves two stages: sampling from the estimated marginal, followed by Monte Carlo approximation of the outgoing message. NBP uses mixture of Gaussians to approximate the continuous potential functions of the graph. For each iteration, the parameters of the mixture of Gaussians are recomputed using Gibbs sampling. The computational complexity for each node is $O(dkM^2)$, where d is the degree of the node, M the number of samples and k the fixed iteration number of the Gibbs sampler. To ensure good approximation, the Gibbs sampler require a large number of particles (a typical setting is $M = 100$ and $\kappa = 100$, which make the NBP algorithm inevitably slow. According to (Sudderth et al, 2004), with 200

particles, the matlab implementation requires about one minute for each NBP iteration.

Repeatedly sampling from products of mixture of Gaussians makes the algorithm computationally very expensive. To tackle this problem we embed Continuously Adaptive Mean Shift (CAMSHIFT) algorithm into NBP to drive the samples around the more likely locations, meanwhile its scalable window size increases the accuracy of projected rigid hand component size. Actually our method merge the “indistinguishable” component by mode detection we can achieve a much more compact ($N' \ll N$) approximation of the products of the messages represented as mixture of Gaussians. (Suppose that the approximate density has N' unique modes and N is the total number of the components of d input mixtures of M Gaussians).

Instead of approximating the products of d messages in one step, the sequential density approximation achieves the compact Gaussian mixture representation by $d-1$ step. That is, first multiply two messages represented as the Gaussians mixtures of M components and apply above density approximation algorithm. The approximated compact representation is then multiplied with the third nonparametric messages. The density approximation is applied again. The above procedure is repeated until the d th nonparametric message is multiplied and approximated. The complexity of sequential density approximation is $O((d-1)M^4)$, which is quite acceptable. With CAMSHIFT method and the sequential density mode propagation, the sampling procedure focus on the feasible configuration space leading to efficient inference over the articulated hand model.

4 EXPERIMENTAL RESULTS

We test our method by tracking hand with no special marker from monocular image sequences in an indoor environment. Quantitative comparison of hand motion angles is performed with “ground truth” from 5DT Cyber Glove. Figure 6 depicts the differences between our tracking results and the ground truth. Since the 5DT Cyber Glove does not provide the function of measuring the displacement of the hand movement, the tracking results are presented in Figure 3, 4, 5 intuitively without the corresponding quantitative analysis.

For notational convenience, we define a belief propagation order: from the fingertip to the palm is “forward” and the inverse is “backward”. In this

paper, we perform message update forward and then backward because the message update order influences the tracking results according to the efficient belief propagation. Each hand joint placed in global coordinate frame enables the joints observation to operate independently while the whole hand is assembled by the process of graphical model inference.

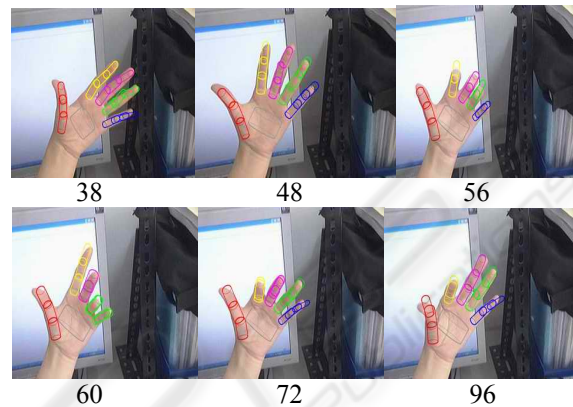


Figure 3: The first tracking results are at the time of 38, 48, 56, 60, 72, 96 frame.

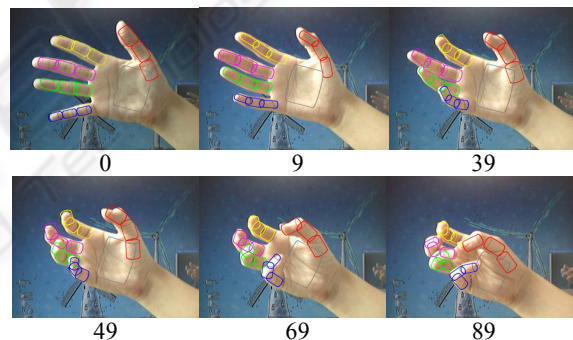


Figure 4: The second tracking results are at the time of 0, 9, 39, 49, 69, 89 frame.

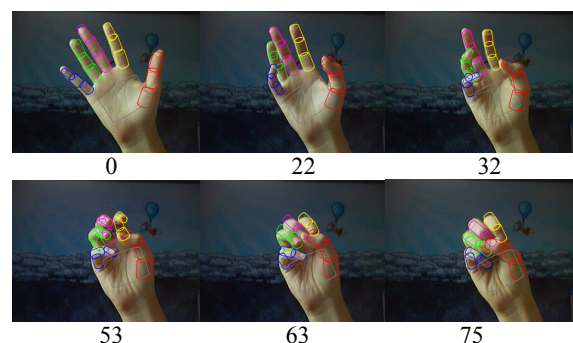


Figure 5: The third tracking results are at the time of 0, 22, 32, 53, 63, 75 frame.

The comparisons between tracking results from the first image series shown in figure 3 and ground truth from 5DT Cyber Glove are shown in Figure 6.

The NBP in feasible configuration space based articulated 3D tracker can achieve 2.5 frames/second in average for the shown 320×240 image series on a Pentium (R) D 3.4G desktop.

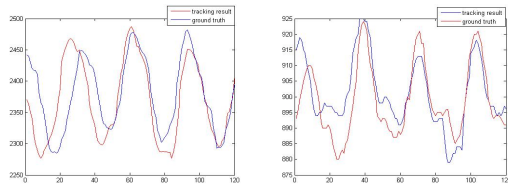


Figure 6: The comparison between our tracking results of figure 3 and the ground truth. The abscissa represents training data (frames), the ordinate represents phalange's angle. (left) distal phalanx of middle finger, (right) distal phalanx of little finger.

5 CONCLUSIONS

Due to the high dimensionality of human hand incurring complexity of hand tracking, graphical models are widely used to decompose multivariate, joint distributions into a set of local interactions. In addition to the traditional physiological constraints and temporal information, we also introduce occlusion constraints of hand motion. The advantage of this framework is that self occlusion could be partially solved. Consequently, the hand tracking is transformed into an inference of graphical model.

We utilize embedded sequential mode propagation underlying NBP in a restrict hand motion space obtained by CAMSHIFT to perform hand tracking. It accelerates tracking procedure remarkably. The experiment results show the capability of the entire framework.

REFERENCES

- Wu, Y., Lin, J., Huang, T. S., December 2005. Analyzing and Capturing Articulated Hand Motion in Image Sequences. In *Vol. 27, No. 12, IEEE Transactions on Pattern Analysis and Machine Intelligence*.
- Stenger, B., Wu, Y., Mendonca, P. R. S., 2001. Model-based 3D tracking of an articulated hand. In *pp. 310-315, Vol. 2, Proc. IEEE Conf. Computer Vision and Pattern Recognition*.
- Wu, Y., Lin, J. Y., Huang, T. S., 2001. Capturing natural hand articulation. In *pp. 426-432, Vol. 2, Proc. IEEE Int. Conf. Computer Vision*.
- Isard, M., Blake, A., 1998. CONDENSATION — conditional density propagation for visual tracking. In *pp. 5-28, Vol. 29, International Journal of Computer Vision*.
- Sudderth, E. B., Mandel, M. I., Freeman, W. T., Willisky, A. S., May 2004. Visual Hand Tracking Using Nonparametric Belief Propagation. In *MIT Laboratory For Information & Decision Systems Technical Report*.
- Lin, J. Y., Wu, Y., Huang, T. S., December 2002. Capturing Human Hand Motion in Image Sequences. In *pp. 99-104, Proc. IEEE Workshop Motion and Video Computing*.
- Chao, E., An, K., Cooney, W., Linscheid, R., 1989. Biomechanics of the Hand: A Basic Research Study. In *Mayo Foundation, Minn.: World Scientific*.
- Tony, X. H., Ning, H. Z., Huang, T. S., 2006. Efficient Nonparametric Belief Propagation with Application to Articulated Body Tracking. In *pp. 214-221, Vol. 1, Proc IEEE Conf. Computer Vision and Pattern Recognition*.
- Isard, M., 2003. PAMPAS: Real-Valued Graphical Models for Computer Vision. In *pp. 18-20, Vol. 1, Proc IEEE Conf. Computer Vision and Pattern Recognition*.
- Sigal, S., Bhatia, S., Roth, S., Black, M. J., Isard, M., 2004. Tracking Loose-limbed People. In *pp. 421-428, Vol. 1, Proc IEEE Conf. Computer Vision and Pattern Recognition*.
- Frey, B. J., Bhatia, S., MacKay, D. J. C., 1998. A revolution: Belief propagation in graphs with cycles. In *pp. 479-485, Vol. 1, Neural Information Processing Systems 10, MIT Press*.
- Wu, Y., Huang, T. S., May 2001. Hand modeling, analysis, and recognition. In *pp. 51-60, IEEE Signal Proc. Mag.*
- Stenger, B. J., Mendonca, P. R. S., Cipolla, R., 2001. Model-based 3D tracking of an articulated hand. In *pp. 310-315, Vol. 2, Proc IEEE Conf. Computer Vision and Pattern Recognition*.